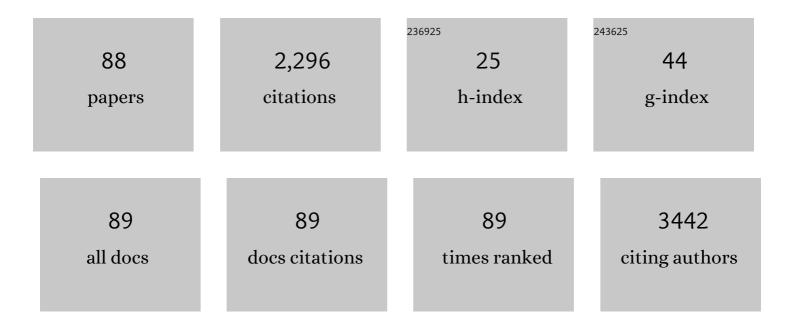
Alois Martin Sprinkart

List of Publications by Year in descending order

Source: https://exaly.com/author-pdf/3082755/publications.pdf Version: 2024-02-01



| # | Article | IF | CITATIONS |
|----|---|-----|-----------|
| 1 | Acute Myocarditis: Multiparametric Cardiac MR Imaging. Radiology, 2014, 273, 383-392. | 7.3 | 130 |
| 2 | Incremental value of quantitative CMR including parametric mapping for the diagnosis of acute myocarditis. European Heart Journal Cardiovascular Imaging, 2016, 17, 154-161. | 1.2 | 127 |
| 3 | Comparison of Original and 2018 Lake Louise Criteria for Diagnosis of Acute Myocarditis: Results of a Validation Cohort. Radiology: Cardiothoracic Imaging, 2019, 1, e190010. | 2.5 | 118 |
| 4 | Gradient Spin Echo (GraSE) imaging for fast myocardial T2 mapping. Journal of Cardiovascular Magnetic Resonance, 2015, 17, 12. | 3.3 | 113 |
| 5 | Comparison between modified Dixon MRI techniques, MR spectroscopic relaxometry, and different histologic quantification methods in the assessment of hepatic steatosis. European Radiology, 2015, 25, 2869-2879. | 4.5 | 106 |
| 6 | Quantification of Liver Fibrosis at T1 and T2 Mapping with Extracellular Volume Fraction MRI: Preclinical Results. Radiology, 2018, 288, 748-754. | 7.3 | 96 |
| 7 | Comprehensive Cardiac Magnetic Resonance for Shortâ€Term Followâ€Up in Acute Myocarditis. Journal of the American Heart Association, 2016, 5, . | 3.7 | 86 |
| 8 | Cardiac Magnetic Resonance Reveals Signs of Subclinical Myocardial Inflammation in Asymptomatic HIV-Infected Patients. Circulation: Cardiovascular Imaging, 2016, 9, e004091. | 2.6 | 83 |
| 9 | Diffuse Myocardial Inflammation in COVID-19 Associated Myocarditis Detected by Multiparametric Cardiac Magnetic Resonance Imaging. Circulation: Cardiovascular Imaging, 2020, 13, e010897. | 2.6 | 79 |
| 10 | N-Acetylaspartylglutamate (NAAG) and N-Acetylaspartate (NAA) in Patients With Schizophrenia. Schizophrenia Bulletin, 2013, 39, 197-205. | 4.3 | 63 |
| 11 | Diffusion-Weighted Magnetic Resonance Imaging of the Pancreas. Investigative Radiology, 2014, 49, 93-100. | 6.2 | 63 |
| 12 | Quantification of fat and skeletal muscle tissue at abdominal computed tomography: associations between single-slice measurements and total compartment volumes. Abdominal Radiology, 2019, 44, 1907-1916. | 2.1 | 63 |
| 13 | Body composition analysis using CT and MRI: intra-individual intermodal comparison of muscle mass and myosteatosis. Scientific Reports, 2020, 10, 11765. | 3.3 | 53 |
| 14 | Feature-tracking myocardial strain analysis in acute myocarditis: diagnostic value and association with myocardial oedema. European Radiology, 2017, 27, 4661-4671. | 4.5 | 50 |
| 15 | Intravoxel incoherent motion model-based liver lesion characterisation from three b-value diffusion-weighted MRI. European Radiology, 2013, 23, 2773-2783. | 4.5 | 49 |
| 16 | Intensity-modulated radiotherapy of the prostate: Dynamic ADC monitoring by DWI at 3.0T. Radiotherapy and Oncology, 2014, 113, 115-120. | 0.6 | 46 |
| 17 | Dynamic and simultaneous MR measurement of <i>R</i> ₁ and <i>R</i> ₂ * changes during respiratory challenges for the assessment of blood and tissue oxygenation. Magnetic Resonance in Medicine, 2013, 70, 136-146. | 3.0 | 45 |
| 18 | Postinterventional Passive Expansion of Partially Dilated Transjugular Intrahepatic Portosystemic Shunt Stents. Journal of Vascular and Interventional Radiology, 2015, 26, 388-394. | 0.5 | 42 |

| # | Article | IF | CITATIONS |
|----|--|------|-----------|
| 19 | 3D-Dixon MRI based volumetry of peri- and epicardial fat. International Journal of Cardiovascular Imaging, 2016, 32, 291-299. | 1.5 | 41 |
| 20 | Left Ventricular Myocardial Fibrosis, Atrophy, and Impaired Contractility in Patients With Pulmonary Arterial Hypertension and a Preserved Left Ventricular Function. Journal of Thoracic Imaging, 2017, 32, 36-42. | 1.5 | 40 |
| 21 | Proton density fat fraction MRI of vertebral bone marrow: Accuracy, repeatability, and reproducibility among readers, field strengths, and imaging platforms. Journal of Magnetic Resonance Imaging, 2019, 50, 1762-1772. | 3.4 | 37 |
| 22 | Fully Automated Segmentation of Connective Tissue Compartments for CT-Based Body Composition Analysis. Investigative Radiology, 2020, 55, 357-366. | 6.2 | 36 |
| 23 | Myocardial Fibrosis and Inflammation in Liver Cirrhosis: MRI Study of the Liver-Heart Axis. Radiology, 2020, 297, 51-61. | 7.3 | 34 |
| 24 | Fat-free muscle area measured by magnetic resonance imaging predicts overall survival of patients undergoing radioembolization of colorectal cancer liver metastases. European Radiology, 2019, 29, 4709-4717. | 4.5 | 26 |
| 25 | Quantitative liver MRI including extracellular volume fraction for non-invasive quantification of liver fibrosis: a prospective proof-of-concept study. Gut, 2018, 67, 593-594. | 12.1 | 25 |
| 26 | Opportunistic Computed Tomography Imaging for the Assessment of Fatty Muscle Fraction Predicts Outcome in Patients Undergoing Transcatheter Aortic Valve Replacement. Circulation, 2020, 141, 234-236. | 1.6 | 25 |
| 27 | Comparison of magnetic resonance feature tracking with harmonic phase imaging analysis (CSPAMM) for assessment of global and regional diastolic function. European Journal of Radiology, 2015, 84, 100-107. | 2.6 | 24 |
| 28 | Accurate IVIM model-based liver lesion characterisation can be achieved with only three b-value DWI. European Radiology, 2018, 28, 4418-4428. | 4.5 | 24 |
| 29 | Effects of a 24â€hrâ€shiftâ€related shortâ€term sleep deprivation on cardiac function: A cardiac magnetic resonanceâ€based study. Journal of Sleep Research, 2019, 28, e12665. | 3.2 | 24 |
| 30 | Yttrium-90 radioembolization for hepatocellular carcinoma: Outcome prediction with MRI derived fat-free muscle area. European Journal of Radiology, 2020, 125, 108889. | 2.6 | 24 |
| 31 | Evaluation of a Simplified Intravoxel Incoherent Motion (IVIM) Analysis of Diffusion-Weighted Imaging for Prediction of Tumor Size Changes and Imaging Response in Breast Cancer Liver Metastases Undergoing Radioembolization. Medicine (United States), 2016, 95, e3275. | 1.0 | 23 |
| 32 | Differentiation of prostatitis and prostate cancer using the Prostate Imaging—Reporting and Data System (PI-RADS). European Journal of Radiology, 2016, 85, 1304-1311. | 2.6 | 23 |
| 33 | The effects of extracellular contrast agent (Gadobutrol) on the precision and reproducibility of cardiovascular magnetic resonance feature tracking. Journal of Cardiovascular Magnetic Resonance, 2016, 18, 30. | 3.3 | 22 |
| 34 | Cardiac MRI Depicts Immune Checkpoint Inhibitor–induced Myocarditis: A Prospective Study. Radiology, 2021, 301, 602-609. | 7.3 | 22 |
| 35 | 3D-Dixon cardiac magnetic resonance detects an increased epicardial fat volume in hypertensive men with myocardial infarction. European Journal of Radiology, 2016, 85, 936-942. | 2.6 | 21 |
| 36 | Detection of liver cirrhosis in standard T2-weighted MRI using deep transfer learning. European Radiology, 2021, 31, 8807-8815. | 4.5 | 21 |

| # | Article | IF | CITATIONS |
|----|---|-----|-----------|
| 37 | End-to-end automated body composition analyses with integrated quality control for opportunistic assessment of sarcopenia in CT. European Radiology, 2022, 32, 3142-3151. | 4.5 | 20 |
| 38 | Quantitative assessment of systolic and diastolic function in patients with LGE negative systemic amyloidosis using CMR. International Journal of Cardiology, 2017, 232, 336-341. | 1.7 | 19 |
| 39 | Multiparametric cardiovascular magnetic resonance imaging in acute myocarditis: a comparison of different measurement approaches. Journal of Cardiovascular Magnetic Resonance, 2019, 21, 54. | 3.3 | 19 |
| 40 | Intravoxel incoherent motion model–based analysis of diffusion-weighted magnetic resonance imaging with 3 b -values for response assessment in locoregional therapy of hepatocellular carcinoma. OncoTargets and Therapy, 2016, Volume 9, 6425-6433. | 2.0 | 17 |
| 41 | Influence of hydration status on cardiovascular magnetic resonance myocardial T1 and T2 relaxation time assessment: an intraindividual study in healthy subjects. Journal of Cardiovascular Magnetic Resonance, 2020, 22, 63. | 3.3 | 14 |
| 42 | Deep Learning-Based Body Composition Analysis Predicts Outcome in Melanoma Patients Treated with Immune Checkpoint Inhibitors. Diagnostics, 2021, 11, 2314. | 2.6 | 13 |
| 43 | Deep learning supports the differentiation of alcoholic and other-than-alcoholic cirrhosis based on MRI. Scientific Reports, 2022, 12, 8297. | 3.3 | 13 |
| 44 | Proton magnetic resonance spectroscopy in focal cortical dysplasia at 3 T. Seizure: the Journal of the British Epilepsy Association, 2015, 32, 23-29. | 2.0 | 12 |
| 45 | Epicardial Fat Volume and Aortic Stiffness in Healthy Individuals: A Quantitative Cardiac Magnetic Resonance Study. RoFo Fortschritte Auf Dem Gebiet Der Rontgenstrahlen Und Der Bildgebenden Verfahren, 2016, 188, 853-858. | 1.3 | 12 |
| 46 | Quantification of liver fibrosis: extracellular volume fraction using an MRI bolus-only technique in a rat animal model. European Radiology Experimental, 2019, 3, 22. | 3.4 | 12 |
| 47 | Epicardial fat, left ventricular strain, and T1-relaxation times in obese individuals with a normal ejection fraction. Acta Radiologica, 2019, 60, 1251-1257. | 1.1 | 12 |
| 48 | Magnetic resonance parametric mapping of the spleen for non-invasive assessment of portal hypertension. European Radiology, 2021, 31, 85-93. | 4.5 | 12 |
| 49 | 1.5 vs 3 Tesla Magnetic Resonance Imaging. Investigative Radiology, 2021, 56, 680-691. | 6.2 | 12 |
| 50 | Non-invasive assessment of liver fibrosis in autoimmune hepatitis: Diagnostic value of liver magnetic resonance parametric mapping including extracellular volume fraction. Abdominal Radiology, 2021, 46, 2458-2466. | 2.1 | 11 |
| 51 | Feasibility of CT-derived myocardial strain measurement in patients with advanced cardiac valve disease. Scientific Reports, 2021, 11, 8793. | 3.3 | 11 |
| 52 | The value of intravoxel incoherent motion model-based diffusion-weighted imaging for outcome prediction in resin-based radioembolization of breast cancer liver metastases. OncoTargets and Therapy, 2016, Volume 9, 4089-4098. | 2.0 | 10 |
| 53 | Intravoxel Incoherent Motion Diffusion-Weighted MR Imaging for Prediction of Early Arterial Blood Flow Stasis in Radioembolization of Breast Cancer Liver Metastases. Journal of Vascular and Interventional Radiology, 2016, 27, 1320-1328. | 0.5 | 10 |
| 54 | Interrelations of Epicardial Fat Volume, Left Ventricular T1-Relaxation Times and Myocardial Strain in Hypertensive Patients. Journal of Thoracic Imaging, 2017, 32, 169-175. | 1.5 | 10 |

| # | Article | IF | CITATIONS |
|----|---|-----|-----------|
| 55 | Cardiac magnetic resonance based evaluation of aortic stiffness and epicardial fat volume in patients with hypertension, diabetes mellitus, and myocardial infarction. Acta Radiologica, 2018, 59, 65-71. | 1.1 | 10 |
| 56 | Multiparametric cardiac magnetic resonance imaging in pediatric and adolescent patients with acute myocarditis. Pediatric Radiology, 2021, 51, 2470-2480. | 2.0 | 10 |
| 57 | Extraretinal Induced Visual Sensations during IMRT of the Brain. PLoS ONE, 2015, 10, e0123440. | 2.5 | 9 |
| 58 | An in vivo comparison of the DREAM sequence with current RF shim technology. Magnetic Resonance Materials in Physics, Biology, and Medicine, 2015, 28, 185-194. | 2.0 | 9 |
| 59 | Revised PROPELLER for T2-weighted imaging of the prostate at 3 Tesla: impact on lesion detection and PI-RADS classification. European Radiology, 2018, 28, 24-30. | 4.5 | 9 |
| 60 | Diagnostic Accuracy of Quantitative Imaging Biomarkers in the Differentiation of Benign and Malignant Vertebral Lesions. Clinical Neuroradiology, 2021, 31, 1059-1070. | 1.9 | 9 |
| 61 | Assessment of cardiac dyssynchrony by cardiac MR: A comparison of velocity encoding and feature tracking analysis. Journal of Magnetic Resonance Imaging, 2016, 43, 940-946. | 3.4 | 8 |
| 62 | CT fatty muscle fraction as a new parameter for muscle quality assessment predicts outcome in venovenous extracorporeal membrane oxygenation. Scientific Reports, 2020, 10, 22391. | 3.3 | 8 |
| 63 | Characterization of the failing murine heart in a desmin knock-out model using a clinical 3ÂT MRI scanner. International Journal of Cardiovascular Imaging, 2012, 28, 1699-1705. | 1.5 | 7 |
| 64 | Comparison of magnetic resonance feature tracking with CSPAMM HARP for the assessment of global and regional layer specific strain. International Journal of Cardiology, 2017, 244, 340-346. | 1.7 | 6 |
| 65 | Short-Term Measurement Repeatability of a Simplified Intravoxel Incoherent Motion (IVIM) Analysis for Routine Clinical Diffusion-Weighted Imaging in Malignant Liver Lesions and Liver Parenchyma at 1.5 T. RoFo Fortschritte Auf Dem Gebiet Der Rontgenstrahlen Und Der Bildgebenden Verfahren, 2019, 191, 199-208. | 1.3 | 6 |
| 66 | Diagnostic value of magnetic resonance parametric mapping for non-invasive assessment of liver fibrosis in patients with primary sclerosing cholangitis. BMC Medical Imaging, 2021, 21, 65. | 2.7 | 6 |
| 67 | Ultrafast volumetric B1+mapping for improved radiofrequency shimming in 3 tesla body MRI. Journal of Magnetic Resonance Imaging, 2014, 40, 857-863. | 3.4 | 5 |
| 68 | In-bore transrectal MRI-guided prostate biopsies: Are there risk factors for complications?. European Journal of Radiology, 2016, 85, 2169-2173. | 2.6 | 5 |
| 69 | Evaluation of Exponential ADC (eADC) and Computed DWI (cDWI) for the Detection of Prostate Cancer. RoFo Fortschritte Auf Dem Gebiet Der Rontgenstrahlen Und Der Bildgebenden Verfahren, 2018, 190, 758-766. | 1.3 | 5 |
| 70 | Is liver lesion characterisation by simplified IVIM DWI also feasible at 3.0ÂT?. European Radiology, 2019, 29, 5889-5900. | 4.5 | 5 |
| 71 | Quantitative and Qualitative Assessment of Pulmonary Emphysema with T2-Weighted PROPELLER MRI in a High-Risk Population Compared to Low-Dose CT. RoFo Fortschritte Auf Dem Gebiet Der Rontgenstrahlen Und Der Bildgebenden Verfahren, 2018, 190, 733-739. | 1.3 | 4 |
| 72 | MRI Assessment of Chylous and Nonchylous Effusions: Use of Multipoint Dixon Fat Quantification. Radiology, 2020, 296, 698-705. | 7.3 | 4 |

| # | Article | IF | CITATIONS |
|----|--|-----|-----------|
| 73 | The effects of flip angle optimization on the precision and reproducibility of feature tracking derived strain assessment in contrast enhanced bSSFP cine images. European Journal of Radiology, 2018, 102, 9-14. | 2.6 | 3 |
| 74 | Flip angle optimization for balanced SSFP: Cardiac cine imaging following the application of standard extracellular contrast agent (gadobutrol). Journal of Magnetic Resonance Imaging, 2018, 47, 255-261. | 3.4 | 3 |
| 75 | Synthetic extracellular volume fraction without hematocrit sampling for hepatic applications. Abdominal Radiology, 2021, 46, 4637-4646. | 2.1 | 3 |
| 76 | Association between single-slice and whole heart measurements of epicardial and pericardial fat in cardiac MRI. Acta Radiologica, 2023, 64, 2229-2237. | 1.1 | 3 |
| 77 | Comparison of different ROI analysis methods for liver lesion characterization with simplified intravoxel incoherent motion (IVIM). Scientific Reports, 2021, 11, 22752. | 3.3 | 3 |
| 78 | Peripartum Cardiomyopathy: Diagnostic and Prognostic Value of Cardiac Magnetic Resonance in the Acute Stage. Diagnostics, 2022, 12, 378. | 2.6 | 3 |
| 79 | Combination of Fat-Free Muscle Index and Total Spontaneous Portosystemic Shunt Area Identifies High-Risk Cirrhosis Patients. Frontiers in Medicine, 2022, 9, 831005. | 2.6 | 3 |
| 80 | Cranial stent position is independently associated with the development of TIPS dysfunction. Scientific Reports, 2022, 12, 3559. | 3.3 | 2 |
| 81 | Synchronization and Alignment of Follow-up Examinations: a Practical and Educational Approach Using the DICOM Reference Coordinate System. Journal of Digital Imaging, 2019, 32, 68-74. | 2.9 | 1 |
| 82 | The impact of rheolytic percutaneous mechanical thrombectomy on glomerular filtration rate levels. Journal of Vascular Surgery: Venous and Lymphatic Disorders, 2020, 8, 545-550. | 1.6 | 1 |
| 83 | Simplified intravoxel incoherent motion diffusion-weighted MRI of liver lesions: feasibility of combined two-colour index maps. European Radiology Experimental, 2021, 5, 33. | 3.4 | 1 |
| 84 | Feature-tracking-based strain analysis – a comparison of tracking algorithms. Polish Journal of Radiology, 2020, 85, 97-103. | 0.9 | 1 |
| 85 | Assessment of liver cirrhosis severity with extracellular volume fraction MRI. Scientific Reports, 2022, 12, . | 3.3 | 1 |
| 86 | Dynamic and simultaneous MR measurement of <i>R</i> ₁ and <i>R</i> ₂ * changes during respiratory challenges for the assessment of blood and tissue oxygenation. Magnetic Resonance in Medicine, 2013, 70, spcone. | 3.0 | 0 |
| 87 | Messung von Fettgehalt und Fettvolumen mittels 1H-MR-spektroskopischer Relaxometrie und quantitativer MR-Bildgebung. TM Technisches Messen, 2016, 83, 257-265. | 0.7 | 0 |
| 88 | Epicardial adipose tissue, aortic stiffness and myocardial fibrosis in healthy individuals: a quantitative cardiac magnetic resonance study. Journal of Cardiovascular Magnetic Resonance, 2016, 18, Q4. | 3.3 | 0 |